

# $\gamma\delta$ TCR immunoglobulin constant region domain exchange in human $\alpha\beta$ TCRs improves TCR pairing without altering TCR gene-modified T cell function

CHANGLI TAO, HONGWEI SHAO, WENFENG ZHANG, HUABEN BO,  
FENGLIN WU, HAN SHEN and SHULIN HUANG

Guangdong Province Key Laboratory for Biotechnology Drug Candidates,  
School of Biosciences and Biopharmaceutics, Guangdong Pharmaceutical University, Guangzhou  
Higher Education Mega Center, Guangzhou, Guangdong 510006, P.R. China

Received January 1, 2016; Accepted December 12, 2016

DOI: 10.3892/mmr.2017.6206

**Abstract.** The adoptive genetic transfer of T cell receptors (TCRs) has been shown to be overall feasible and offer clinical potential as a treatment for different types of cancer. However, this promising clinical approach is limited by the serious potential consequence that exogenous TCR mispairing with endogenous TCR chains may lead to the risk of self-reactivity. In the present study, domain-exchange and three-dimensional modeling strategies were used to create a set of chimeric TCR variants, which were used to exchange the partial or complete constant region of  $\alpha\beta$ TCR with corresponding  $\gamma\delta$ TCR domains. The expression, assembly and function of the chimeric TCR variants were examined in Jurkat T cells and peripheral mononuclear blood cells (PBMCs). Genetically-encoded chimeras were fused with a pair of fluorescent proteins (ECFP/EYFP) to monitor expression and the pairing between chimeric TCR $\alpha$  chains and TCR $\beta$  chains. The fluorescence energy transfer based on confocal laser scanning microscopy showed that the introduction of  $\gamma\delta$ TCR constant sequences into the  $\alpha\beta$ TCR did not result in a global reduction of mispairing with endogenous TCR. However, the TCR harboring the immunoglobulin-like domain of the  $\gamma\delta$ TCR constant region (i.e., TCR $\Delta$ IgC), showed a higher expression and preferential pairing, compared with wild-type (wt)TCR. The function analysis showed that TCR $\Delta$ IgC exhibited the same levels of interferon- $\gamma$  production and cytotoxic activity, compared with wtTCR. Furthermore, these

modified TCR-transduced T cells retained the classic human leukocyte antigen restriction of the original TCR. The other two chimeric TCRs, had either exchange of the cp+tm+ic domain or exchange of the whole C domain (Fig. 1). Ultimately, exchange of these domains demonstrated defective function in the transduced T cells. Taken together, these findings may provide further understanding of the  $\gamma\delta$ TCR constant domain with implications for the improvement of TCR gene transfer therapy.

## Introduction

In previous years, the potency of genetically modified T cell-mediated immunity against viruses and certain malignancies has been well established. TCR gene adoptive therapy is a clinically promising approach for the treatment of malignant tumors and viral diseases. Using *ex vivo* gene transfer, T cells isolated from patients can be genetically engineered to express a novel TCR, and the engineered T cells are re-infused back into the patient to specifically recognize a tumor-associated antigen and thereby selectively lyse tumor cells (1). However toxicity has been observed in clinical trials using genetically modified TCR therapies (2). An important toxic effect is on-target off-tumor activity, which occurs if the peptide target sequence of the TCR is also expressed on other cells (3), which has been reported to occur in clinical trials (4-6). Another undesirable toxic effect is off-target reactivity, and one cause for this effect is the occurrence of cross-reactivity, which is due to the ability of the TCR to react against the peptides expressed on non-target proteins (7). This toxic effect may also result from the mixture of TCRs generated by the introduced TCR  $\alpha$ - and  $\beta$ -chains mispairing with the endogenous TCR  $\beta$ - and  $\alpha$ -chains. The mispaired TCR increases the risk of unknown specificity causing autoreactivity (8). No formal observations of toxicities mediated by TCR mispairing have been observed in clinical trials to date, however, preclinical studies have demonstrated that mispaired TCRs have the potential to induce the harmful recognition of self-antigens, resulting in graft, vs. host disease (9). These findings indicate the requirement to prevent or reduce TCR mispairing, to

---

*Correspondence to:* Professor Shulin Huang, Guangdong Province Key Laboratory for Biotechnology Drug Candidates, School of Biosciences and Biopharmaceutics, Guangdong Pharmaceutical University, Guangzhou Higher Education Mega Center, 280 East Road, Guangzhou, Guangdong 510006, P.R. China  
E-mail: shulhuang@sina.com

**Key words:** T cell receptor, mispairing,  $\gamma\delta$ T cell receptor, fluorescence resonance energy transfer, T cell receptor gene therapy

improve T cell avidity and reduce potential off-target toxicity, including the genetic modification of TCR transgenes (10-13), disruption of endogenous TCR chains via short hairpin RNA or zinc finger nucleases (14,15),  $\alpha\beta$  TCR transfer to  $\gamma\delta$ T cells or  $\gamma\delta$ 2TCR transduction of  $\alpha\beta$ T cells (16,17).

Although it has been reported that the transfer of  $\gamma\delta$ 2TCR into  $\alpha\beta$ T cells can prevent the formation of mixed TCR dimers and efficiently kill cancer cell lines *in vitro* (17), the role of the V $\gamma$ 9V $\delta$ 2 TCR in antigen recognition remains to be fully elucidated, as does the biology of  $\gamma\delta$ TCR, compared with  $\alpha\beta$ TCR. Thus, the present study aimed to examine whether the domains of the  $\gamma\delta$ TCR constant exchanged in  $\alpha\beta$ TCR can improve the pairing and function of  $\alpha\beta$ TCR. Three chimeric TCR variants were constructed, and domain-exchange and three-dimensional (3D) modeling strategies were applied, in which the  $\alpha\beta$ TCR constant was replaced with partial or complete constant regions of  $\gamma\delta$ TCR, leaving the variable domains intact. Subsequently, genetically-encoded reporters coupled with a pair of fluorescent proteins were constructed to monitor the expression and pairing between chimeric TCR $\alpha$  chains and TCR $\beta$  chains using a confocal laser scanning microscope (CLSM) in living cells. The data showed that swapping of the  $\alpha\beta$ TCR constant region of immunoglobulin-like (Ig) domain for the corresponding  $\gamma\delta$ TCR domain enhanced expression and reduced mispairing on the cell surface. The other two chimeric TCRs harboring the connecting peptide, transmembrane and intracellular (cp+tm+ic) domains or complete constant (C) domain of  $\gamma\delta$ TCR did not show improved expression, however, the level of mispairing decreased. Finally the function of the chimeric TCR variants were examined in peripheral blood mononuclear cells (PBMCs), which revealed that the introduction of  $\gamma\delta$ TCR constant region of Ig domains in the  $\alpha\beta$ TCR was able to mediate the same levels of interferon (IFN)- $\gamma$  secretion and cytotoxic activity as the wild-type (wt)TCR when co-cultured with human leukocyte antigen (HLA)<sup>2+</sup> human hepatocellular cell lines. However, the other two TCRs containing the  $\gamma\delta$ TCR cp+tm+ic domains or C domains did not trigger the lymphocytes to produce IFN- $\gamma$  or activate cytotoxic T cells when co-cultured with HLA-A<sup>2+</sup> or HLA-A<sup>2-</sup> target cells. Taken together, these findings demonstrated that exchange of the constant region of the Ig domain of  $\gamma\delta$ TCR in  $\alpha\beta$ TCR decreased mispairing without compromising T cell function, however, this was not the case in those containing the  $\gamma\delta$ TCR cp+tm+ic or C domains.

## Materials and methods

**Cells.** PBMCs of HLA-A<sup>2+</sup> were isolated from the blood of healthy donors (Table I), following the provision of informed consent, using Ficoll gradient centrifugation at 600 x g for 20 min at room temperature, followed by washing in PBS, re-suspension at a concentration of 1x10<sup>6</sup> cells/ml and activated by soluble anti-CD3 $\epsilon$  mAb (OKT3, 30 ng/ml, R&D Systems, Inc., Minneapolis, MN, USA) and soluble anti-CD28 mAb (1 ng/ml, R&D Systems, Inc.) and 300 IU/ml recombinant human IL-2 (R&D Systems, Inc.) at 37°C for 48 h. Human PBMCs and Jurkat/E6-1 cells (cat. no. TIB-152; American Type Culture Collection, Manassas, VA, USA) were cultured in RPMI-1640 medium (Gibco; Thermo Fisher Scientific, Inc., Waltham, MA, USA) supplemented with 10% FBS (Gibco;

Thermo Fisher Scientific, Inc.) and 100 U/ml penicillin-streptomycin at 37°C and 5% CO<sub>2</sub>.

The HEK293 human embryonic kidney cell line, and the HepG2 (HLA-A<sup>2+</sup>), Huh-1 (HLA-A<sup>2+</sup>) and BEL-7402 (HLA-A<sup>2-</sup>) human hepatocellular carcinoma cell lines (Guangdong Province Key Laboratory for Biotechnology Drug Candidates, Guangzhou, China) were cultured in DMEM (Gibco; Thermo Fisher Scientific, Inc.) supplemented with 10% FBS (Gibco; Thermo Fisher Scientific, Inc.) and 100 U/ml penicillin-streptomycin at 37°C and 5% CO<sub>2</sub>.

**Vector construction.** The  $\alpha\beta$ TCR was isolated from tumor-infiltrating lymphocytes of a patient (HLA-A<sup>2+</sup>;  $\alpha$ -fetoprotein<sup>+</sup>) with hepatocellular carcinoma, which was preserved in our laboratory, as described previously (Table II) (18). The  $\gamma\delta$ 2TCR was isolated from healthy human PBMCs and was composed of TRGV9/J2/C1 and TRDV2/D3/J1/C1. TCR-V(D)J gene nomenclature was according to <http://www.imgt.org>. Unmodified wtTCR was used as a control TCR.

Three TCR variants were constructed using a domain-exchange strategy in which the IgC, cp+tm+ic and C regions of  $\alpha\beta$ TCR were exchanged for corresponding regions of  $\gamma\delta$ TCR. These three chimeras were termed TCR $\Delta$ IgC; TCR $\Delta$ cp+tm+ic; and TCR $\Delta$ C, respectively.  $\Delta$  indicates a lack of  $\alpha\beta$ TCR domain/s and replacement by corresponding  $\gamma\delta$ TCR domain/s. The exact boundaries of the IgC, cp+tm+ic and C domains of TCR $\alpha$ , TCR $\beta$ , TCR $\gamma$  and TCR $\delta$  are described in the legend of Fig. 1. To measure the pairing between the TCR  $\alpha$ - and  $\beta$ -chains, the three modified TCRs were coupled to a pair of fluorescent proteins, ECFP and EYFP, and adenoviral particles without fluorescent proteins were constructed and produced, as described previously (18). Primer sequences used for cloning the TCR $\alpha$ - and  $\beta$ - fusion genes and TCR are provided in Tables III, IV and V. All TCR constructs were sequence verified.

**Cell transfection.** The TCR variants fused to the pair of ECFP and EYFP fluorescent proteins were transduced into Jurkat cells and BEL-7402 cells at a density of 1x10<sup>6</sup> cells/ml, using Lipofectamine LTX/PLUS (Invitrogen; Thermo Fisher Scientific, Inc.) according to the manufacturer's protocol.

**Image acquisition and fluorescence resonance energy transfer (FRET) analysis.** Confocal images of cells were captured using an Olympus FluoView1000 CLSM with FV10-ASW 1.7 software (Olympus, Tokyo, Japan), and apparent FRET efficiency was calculated, as described previously (18). Briefly, the Jurkat cells transduced with chimeric TCR constructs were immobilized onto a glass-bottomed dish, and the TCR construct-transduced BEL-7402 cells grown on the glass-bottomed dish were washed twice with PBS solution. The ECFP channel was excited with a 458 nm argon laser as a donor and the EYFP channel was excited with a 515 nm argon laser as an acceptor. Subsequently, seven images were captured to calculate FRET efficiency. This was calculated using the sensitized acceptor emission method using the following equation: Efficiency=1-I<sub>DA</sub>/[I<sub>DA</sub>+pFRET $\times$ [( $\psi_{dd}/\psi_{aa}$ ) $\times$ (Q<sub>d</sub>/Q<sub>a</sub>)]], where pFRET is the processed FRET obtained by removing the donor SBT (DSBT) and the acceptor SBT (ASBT) from the contaminated or uncorrected FRET; I<sub>DA</sub> is the intensity of the donor in the presence of the acceptor;  $\psi_{dd}$  and  $\psi_{aa}$  are the

Table I. Details of blood donors.

Number	Gender	Age	Hospital admitted to	Dates of blood donation
1	Female	24	The First Affiliated Hospital/School of Clinical Medicine of Guangdong Pharmaceutical University	2013.9.15, 2013.9.21, 2013.9.30, 2013.10.9, 2013.10.20
2	Male	25		2013.9.15
3	Male	30		2013.9.15, 2013.9.21, 2013.9.30, 2013.10.9, 2013.10.20
4	Female	28		2013.9.15
5	Male	21		2013.9.15, 2013.9.21, 2013.9.30, 2013.10.9, 2013.10.20

Table II. Patient details of patient with hepatocellular carcinoma.

Number	Gender	Age	Hospital admitted to	Dates of blood donation
012	Male	54	The First Affiliated Hospital/School of Clinical Medicine of Guangdong Pharmaceutical University	2010.5.9

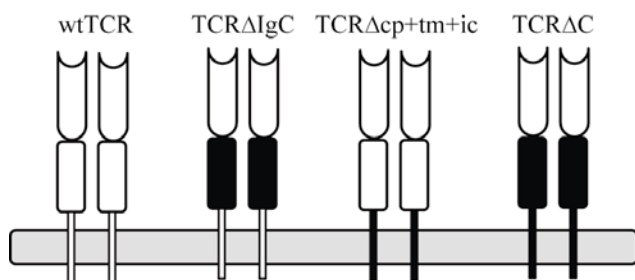


Figure 1. Schematic representation of chimeric TCR variants used in the present study. wtTCRs were isolated from tumor-infiltrating lymphocytes of patients as control TCRs. Three chimeric TCRs constructs were generated by replacement of the either IgC, cp+tm+ic, or C regions of  $\alpha\beta$ TCR (white) by corresponding  $\gamma\delta$ TCR (black). The amino acid boundaries of the domains were as follows: TCR $\Delta$ IgC  $\alpha$  chain (aa132-221) replaced by  $\delta$  chain (aa140-231),  $\beta$  chain (aa136-263) replaced by  $\gamma$  chain (aa140-248); TCR $\Delta$ IgC retained the connecting peptide domains of the  $\alpha$  and  $\beta$  chains. TCR $\Delta$ cp+tm+ic  $\alpha$  chain (aa222-271) replaced by  $\delta$  chain (aa232-292),  $\beta$  chain (aa264-313) replaced by  $\gamma$  chain (aa249-311), TCR $\Delta$ C  $\alpha$  chain (aa132-271) replaced by  $\delta$  chain (aa140-292),  $\beta$  chain (aa136-313) replaced by  $\gamma$  chain (aa140-311). TCR, T cell receptor; wt, wild-type; Ig, immunoglobulin-like; cp+tm+ic, connecting peptide, transmembrane and intracellular; C, complete region.

collection efficiencies in the donor and acceptor channel; and  $Q_d$  and  $Q_a$  are the quantum yield of the donor and acceptor, respectively. Statistical analysis of the mean FRET efficiency were calculated from multiple ( $n=4$ ) cell images in each group and five randomly selected regions of interest (ROI) in each cell image.

#### TCR adenovirus construction and transduction of T cells.

For production of the adenovirus, HEK-293 cells were transfected with the respective TCR-encoding shuttle plasmid and second-generation Ad5F35 adenoviral packaging plasmid (pBHGIoxdelE13Cre; Biovector Science Lab, Inc., Beijing, China). The HEK-293 cells were seeded in 6-well plates at a

density of  $1 \times 10^6$  per well. After 24 h, the cells were co-transfected with an equimolar ratio of the two plasmids ( $2.5 \mu\text{g}$  total DNA per well) and  $6 \mu\text{l/well}$  Lipofectamine 2000 transfection reagent (Invitrogen; Thermo Fisher Scientific, Inc.) according to the manufacturer's protocol. The adenovirus supernatants were harvested ~12 days following transfection, cellular debris was removed by centrifugation at  $14,000 \times g$  for 10 min at room temperature. Adenovirus particle titers were determined using the TCID<sub>50</sub> method and the supernatants were directly used for transduction of the Jurkat T cells and PBMCs, respectively, as previously described (18).

**Flow cytometry and analysis.** The surface expression of the transgenic TCRs on the cells were assessed by fluorescein isothiocyanate (FITC)-conjugated anti-TCRV $\alpha$ 12.1 mAb (cat. no. TCR2764; dilution, 1:500; Invitrogen; Thermo Fisher Scientific, Inc.) and PE-conjugated anti-TCRV $\beta$ 7.1 mAb (cat. no. IM2287; dilution, 1:500; Beckman Coulter, Inc., Brea, CA, USA). The transduced Jurkat T cells and PBMCs ( $5 \times 10^5$ ) were stained with the mAbs on ice for 30 min. Following washing with PBS, the cells were fixed in 2% PFA prior to measurements on an Epics-XL flow cytometer (Beckman Coulter, Inc.). Non-transduced Jurkat T cells and PBMCs were used as controls.

**Cytokine release assays.** The unmodified PBMCs and TCR-modified PBMCs were assessed for reactivity in IFN- $\gamma$  release assays using commercially available ELISA kits (Boster Systems, Inc., Pleasanton, CA, USA). The HepG2 (HLA-A<sup>2+</sup>), Huh-1 (HLA-A<sup>2+</sup>) and BEL-7402 (HLA-A<sup>2+</sup>) target human hepatocellular carcinoma cell lines were cultured in medium at 37°C, followed washing with PBS prior to the initiation of co-cultures. For these assays,  $3 \times 10^5$  responder cells (PBMCs) and  $1 \times 10^4$  stimulator cells were incubated in a 0.2 ml RPMI-1640 medium (Gibco; Thermo Fisher Scientific, Inc.) supplemented with 10% FBS and 100 U/ml

Table III. Primers for amplifying TCR $\beta$  $\Delta$ IgC-EYFP and TCR $\alpha$  $\Delta$ IgC-ECFP fusion genes (regular polymerase chain reaction (PCR) and SOE-PCR).

Gene name	Primer name	Direction	Primer sequence
TRBV	P1	Forward	ATAGCTAGCGCCACCATGGGCTGCAGGCTGCTCTG
	P2	Reverse	ACATCTGCATCAAGTTGTTTCTCCAGTACGGTCAGCCT
TRGC	P3	Forward	AGGCTGACCGTACTGGAGAAACAACCTTGATGCAGATGT
	P4	Reverse	CGGAGGTGAAGCCACAGTCTGTCTTTATTGGAGGAAAG
TRBCm	P5	Forward	CTTTCCTCCAATAAAGACAGACTGTGGCTTCACCTCCG
	P6	Reverse	CTCGCCCTTGCTCACCATGCCTCTGGAATCCTTTCT
EYFP	P7	Forward	AGAAAGGATTCCAGAGGCATGGTGAGCAAGGGCGAG
	P8	Reverse	CGGCCTCGACTTACTTGTACAGCTCGTC
TRAV	X1	Forward	ACGCCACAACCTTGGCCACCATGATATCCTTGAGAGTT
	X2	Reverse	GGTTTGGTATGAGGCTGACTATTTGGTTTTACTGTCAGTCTGG
TRDC	X3	Forward	CCAGACTGACAGTAAAACCAAATAGTCAGCCTCATACCAAACC
	X4	Reverse	GCTTGACATCACAGGAACCTTCTGTAGAATCTGTCTTCACTTC
TRACm	X5	Forward	GAAGTGAAGACAGATTCTACAGAAAGTTCCTGTGATGTCAAGC
	X6	Reverse	CTCCTCGCCCTTGCTCACCATGCTGGACCACAGCCGCAGC
ECFP	X7	Forward	GCTGCGGCTGTGGTCCAGCATGGTGAGCAAGGGCGAGGAG
	X8	Reverse	AGTGCGGCGCGCTTACTTGTACAGCTCGTCCAT

Restriction enzyme sites are underlined. SOE-PCR, splicing by overlap extension-polymerase chain reaction.

Table IV. Primers for amplifying TCR $\beta$  $\Delta$ cp+tm+ic-EYFP and TCR $\alpha$  $\Delta$ cp+tm+ic-ECFP fusion gene (regular polymerase chain reaction (PCR) and SOE-PCR).

Gene	Primer name	Direction	Primer sequence
TRBVC	P1	Forward	ATAGCTAGCGCCACCATGGGCTGCAGGCTGCTCTG
	O2	Reverse	GATCCATTGTGATGACATCTGCTCTACCCCAGGCCTCG
TRGCm	O3	Forward	CGAGGCCTGGGGTAGAGCAGATGTCATCACAATGGATC
	O4	Reverse	CCTCGCCCTTGCTCACCATTGATTTCTCTCCATTGCAG
EYFP	O5	Forward	CTGCAATGGAGAGAAATCAATGGTGAGCAAGGGC
	P8	Reverse	CGGCCTCGACTTACTTGTACAGCTCGTC
TRAVC	X1	Forward	ACGCCACAACCTTGGCCACCATGATATCCTTGAGAGTT
	H2	Reverse	CCTTTGGTTTTACGTGATCTGGGCTGGGGAAGAAGGTG
TRDCm	H3	Forward	CACCTTCTTCCCCAGCCAGATCACGTAACCAAAGG
	H4	Reverse	CCTCGCCCTTGCTCACCATCAAGAAAAATAACTTGGCAGT
ECFP	H5	Forward	ACTGCCAAGTTATTTTCTTGATGGTGAGCAAGGGCGAGG
	X8	Reverse	AGTGCGGCGCGCTTACTTGTACAGCTCGTCCAT

Restriction enzyme sites are underlined. SOE-PCR, splicing by overlap extension-polymerase chain reaction.

penicillin/streptomycin in individual wells of 96-well plates and were co-cultured for 24 h at 37°C and 5% CO<sub>2</sub>. The secretion of IFN- $\gamma$  was measured in the culture supernatants diluted to be in the linear range of the assay.

**CTL assay.** The abilities of the transduced PBMCs to lyse the HLA-A<sup>2+</sup>/HLA-A<sup>2-</sup> human hepatocellular carcinoma targets were measured using a calcein AM (CAM) release assay (Dojindo Molecular Technologies, Inc., Kumamoto, Japan),

as described previously (19). Briefly, 1x10<sup>6</sup> tumor cells were labeled with 2  $\mu$ M CAM, which was diluted from a 1 mM stock solution of CAM in dimethyl sulfoxide (Sigma-Aldrich; Merck Millipore, Darmstadt, Germany) for 30 min at 37°C. The labeled target cells were washed three times with PBS and re-suspended at a concentration of 1x10<sup>5</sup> cells/ml in complete medium. The labeled target cells (1x10<sup>4</sup> in a volume of 100  $\mu$ l) were plated in 96-well V-bottomed plates with effector cells in 200  $\mu$ l of complete medium at effector to



Table V. Primers for amplifying TCR $\beta$  $\Delta$ C-EYFP and TCR $\alpha$  $\Delta$ C-ECFP fusion genes (regular polymerase chain reaction (PCR) and SOE-PCR).

Gene	Primer name	Direction	Primer sequence
TRBV	P1	Forward	ATAGCTAGCGCCACCATGGGCTGCAGGCTGCTCTG
	P2	Reverse	ACATCTGCATCAAGTTGTTTCTCCAGTACGGTCAGCCT
TRGC+GCm	P3	Forward	AGGCTGACCGTACTGGAGAAACAACCTTGATGCAGATGT
	O4	Reverse	CCTCGCCCTTGCTCACCATTGATTTCTCTCCATTGCAG
EYFP	O5	Forward	CTGCAATGGAGAGAAATCAATGGTGAGCAAGGGC
	P8	Reverse	CGGCCTCGACTTACTTGTACAGCTCGTC
TRAV	X1	Forward	ACGCCACAACCTTGGCCACCATGATATCCTTGAGAGTT
	X2	Reverse	GGTTTGGTATGAGGCTGACTATTTGGTTTTACTGTCACTCTGG
TRDC+DCm	X3	Forward	CCAGACTGACAGTAAAACCAAATAGTCAGCCTCATACCAAACC
	H4	Reverse	CCTCGCCCTTGCTCACCATCAAGAAAAATAACTTGGCAGT
ECFP	H5	Forward	ACTGCCAAGTTATTTTTCTTGATGGTGAGCAAGGGCGAGG
	X8	Reverse	AGTGCGGCCGCTTACTTGTACAGCTCGTCCAT

Restriction enzyme sites are underlined. SOE-PCR, splicing by overlap extension-polymerase chain reaction.

target (E:T) ratios between 1:1 and 30:1. Following incubation for 4 h at 37°C with 5% CO<sub>2</sub>, the supernatants was harvested and the quantities of calcein released were measured using a Varioskan Flash multimode reader (Thermo Fisher Scientific, Inc.). Spontaneous release was determined by incubating the target cells in medium alone, and maximum release was determined by suspending the cells with 1% Triton X-100. Each data point was an average of four wells. The percentage of PBMC-specific lysis was calculated as follows: Specific lysis (%)=(experimental release-spontaneous release)/(maximum release-spontaneous release) x 100.

**Splicing by overlap extension (SOE)-PCR.** This method was used to generate the fusion genes of three chimeric TCR variants. Variable fragments for generating TCR $\alpha$  $\Delta$ IgC-ECFP variants (including TCRAV, TRDC, TRACm and ECFP) and TCR $\beta$  $\Delta$ IgC-EYFP variants (including TRBV, TRGC, TRBCm and EYFP) were amplified using a set of forward primers and reverse primers (Table III). The first step of SOE-PCR reactions were performed with 100 ng of the template without primers, 10X Buffer, 2 mM dNTPs, 25 mM MgSO<sub>4</sub>, 0.5 U KOD-Plus-Neo Polymerase (Toyobo Co., Ltd., Osaka, Japan) in 25  $\mu$ l reaction volume. The PCR cycling conditions were as follows: Denaturation at 94°C for 2 min, followed by 5 cycles at 94°C for 30 sec, at 57°C for 30 sec, and at 68°C for 90 sec, and completed with a final extension at 68°C for 7 min. The PCR generated overlapping gene segments that are then used as template DNA for the second step of SOE-PCR to create a full-length product. Therefore, another 25  $\mu$ l reaction mixture (contained 10X Buffer, 2 mM dNTPs, 25 mM MgSO<sub>4</sub>, 0.5 KOD-Plus-Neo Polymerase and 1  $\mu$ M forward primer X1/P1 and reverse primer X8/P8; Invitrogen; Thermo Fisher Scientific, Inc.) were added to the first reaction mixture for the second step of SOE-PCR. The reaction conditions were initial denaturation at 94°C for 2 min, followed by 30 cycles at 94°C for 30 sec, at 62°C for 30 sec, and at 68°C for 90 sec and a final extension at 68°C for 7 min. The other two TCR

(TCR $\Delta$ cp+tm+ic and TCR $\Delta$ C) fusion genes were generate using the same methods, as the primer sequences for the amplification of variable regions and fusion chains are given in Tables IV and V.

**Statistical analysis.** Differences among the TCRs in various assays were examined using Student's t-test (unpaired; two-tailed) and two-way analysis of variance with a Bonferroni's multiple comparisons test using GraphPad Prism 6 software (GraphPad Software Inc., La Jolla, CA, USA). P<0.05 was considered to indicate a statistically significant difference. Data are expressed as the mean  $\pm$  standard deviation.

## Results

**Expression of wtTCR and chimeric TCR constructs.** In the present study, three chimeric TCR variants were generated, in which the IgC, cp+tm+ic and C regions of  $\alpha\beta$ TCR were replaced with corresponding regions of  $\gamma\delta$ TCR (Fig. 1). The wtTCR and chimeric TCR genes were cloned separately into the pDC315 shuttle plasmid to produce the Ad5F35 adenovirus, and transduction of Jurkat T cells was performed with subsequent fluorescence-activated cell sorting analysis. Double immunofluorescent staining with anti-TCRV $\alpha$ 12 mAb<sup>FITC</sup> and anti-V $\beta$ 7mAb<sup>PE</sup> showed that Jurkat cells transduced with TCR $\Delta$ IgC exhibited higher surface coexpression (17.1%), compared with wtTCR (10.7%), and TCR $\Delta$ cp+tm+ic exhibited a marginally higher surface expression (13.4%), compared with wtTCR. By contrast, TCR $\Delta$ C exhibited a lower level of surface expression, compared with wtTCR (Fig. 2). To further examine the expression of the chimeras in living cells, the C terminus of chimeric TCR $\alpha$  chains and TCR $\beta$  chains were fused to a pair of cyan and yellow fluorescent proteins, ECFP and EYFP respectively (Fig. 3A and B). In Jurkat cells, the fluorescence observation using a CLSM showed that TCR $\Delta$ IgC was expressed more markedly on the cell surface, which was in accordance with the flow cytometry results. By

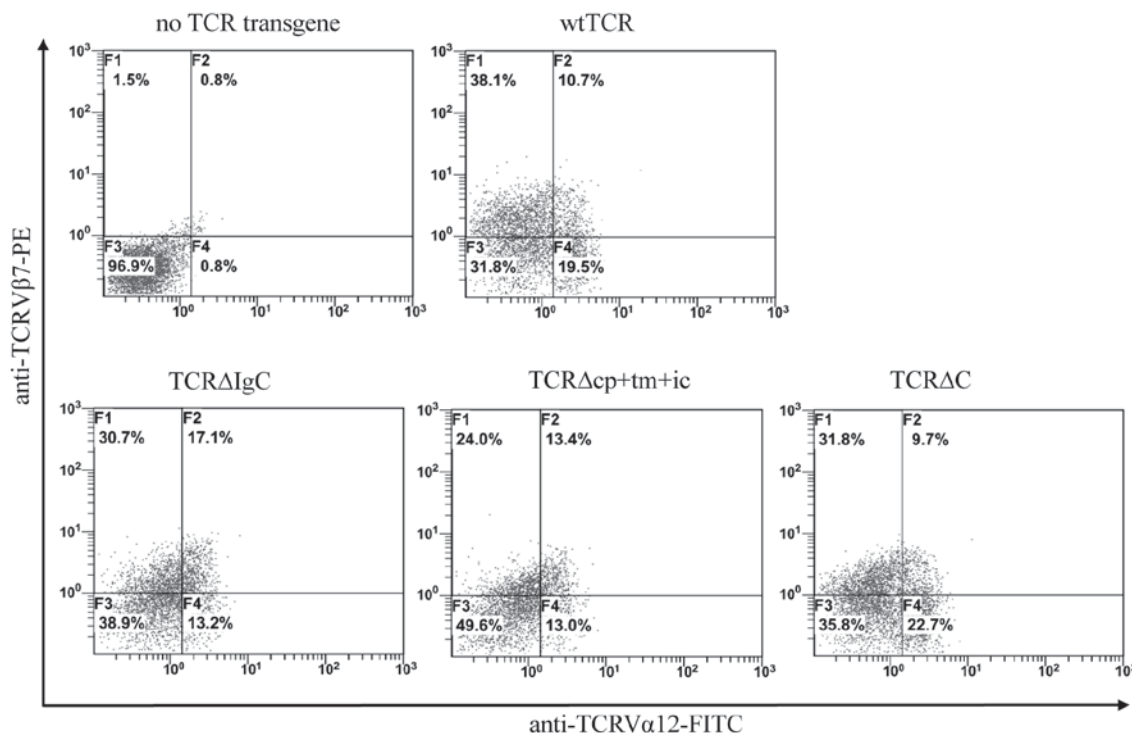


Figure 2. Chimeric TCR variants are expressed in transduced Jurkat cells. Transduced cells stained with anti-TCR Vα12.1 mAb<sup>FITC</sup> and anti-Vβ7.1 mAb<sup>PE</sup>, followed by fluorescence-activated cell sorting analysis to monitor cell surface expression. Representative examples of three individual measurements of one healthy donor are displayed and percentages of double immunofluorescence-stained T cells in upper right quadrants are indicated. TCR, T-cell receptor; wt, wild-type; Ig, immunoglobulin-like; cp+tm+ic, connecting peptide, transmembrane and intracellular.

contrast, the other two modified TCRs, TCRΔcp+tm+ic and TCRΔC, exhibited no apparent difference in expression levels, compared with wtTCR. These data suggested that the modified  $\alpha\beta$ TCRs harboring the  $\gamma\delta$ TCR constant region were expressed on the Jurkat cell surface and that the FRET reporters were able to be used for monitoring the expression and interaction of TCR variants.

**Analysis of TCR mispairing.** The Jurkat cell line (cloneE6-1) was used as a recipient T cell model for TCR gene transfer, to determine whether the chimeric TCRα- and β-chains assembled preferentially when there was a pair of endogenous TCRs. It was hypothesized that the introduced TCR α- and β-chains comprising heterodimers on the cell surface results in FRET efficiency between the donor (ECFP) and acceptor (EYFP) fluorescent proteins. When the introduced TCR α- and β- chains and the endogenous TCR β- and α-chains mispair, FRET is not detected between the mispairing TCRs (Fig. 3C). As shown in Fig. 3A, seven images were used to remove the DSBT and ASBT from the contaminated FRET to obtain the FRET efficiency images. The corrected FRET efficiency images showed that TCRΔIgC exhibited a higher FRET efficiency, compared with wtTCR. The images of TCRΔcp+tm+ic and TCRΔC exhibited no differences in FRET efficiencies, compared with wtTCR. A total of four independent cell images and five ROIs in each cell image were selected for FRET efficiency analysis, respectively, in each group. The statistical results showed that the average FRET efficiency between the TCRΔIgC α- and β-chains ( $10.69 \pm 0.76\%$ ) was significantly higher, compared with the average FRET efficiency between the wtTCR α- and β-chains ( $7.92 \pm 1.32\%$ ;  $P < 0.01$ ). No significant differences

were found between the FRET efficiencies of the other two chimeric TCRs ( $9.07 \pm 0.61$  and  $8.95 \pm 0.89\%$ ), compared with wtTCR ( $P > 0.05$ ; Fig. 3D).

To further investigate the extent of mispairing of the modified TCR with the endogenous TCR, BEL-7402 cells deficient in TCR and CD3 molecules were selected as the next recipient cell model. It was hypothesized that as there was no endogenous TCR in the BEL-7402 cells, the pairing of the introduced TCR α- and β-chains will not be interfered with, allowing the extent of mispairing to be measured by comparing the FRET efficiencies of BEL-7402 and Jurkat cells. The images showed that the TCRΔIgC exhibited a higher FRET efficiency, compared with the wtTCR in the BEL-7402 cells (Fig. 3B). The statistical results showed that the average FRET efficiency of wtTCR in the Jurkat cells ( $7.92 \pm 1.32\%$ ) was lower, compared with that in the BEL-7402 cells ( $10.59 \pm 1.02\%$ ;  $P < 0.05$ ; Fig. 3D), suggesting that the wtTCR was mispaired with the endogenous TCR in Jurkat cells, and the level of mispairing with endogenous TCR was 25%. Statistical analysis also showed that the FRET efficiencies of TCRΔIgC were decreased in the Jurkat cells ( $10.69 \pm 0.76\%$ ), compared with the BEL-7402 cells ( $13.34 \pm 0.40\%$ ), indicating a 20% mismatch rate in the Jurkat cells (Fig. 3D). TCRΔcp+tm+ic and TCRΔC also showed mispairing with the endogenous TCR (19 and 14%, respectively). Together, these data showed that replacement with various constant domains of  $\gamma\delta$ TCR in  $\alpha\beta$ TCR reduced mispairing to the same extent, but were unable to prevent mispairing.

**Analysis of TCR-transduced primary T cells.** The Ad5F35 adenovirus encoding the wtTCR and the chimeric TCRs were used to transfer into PBMCs, and PBMCs expressing the

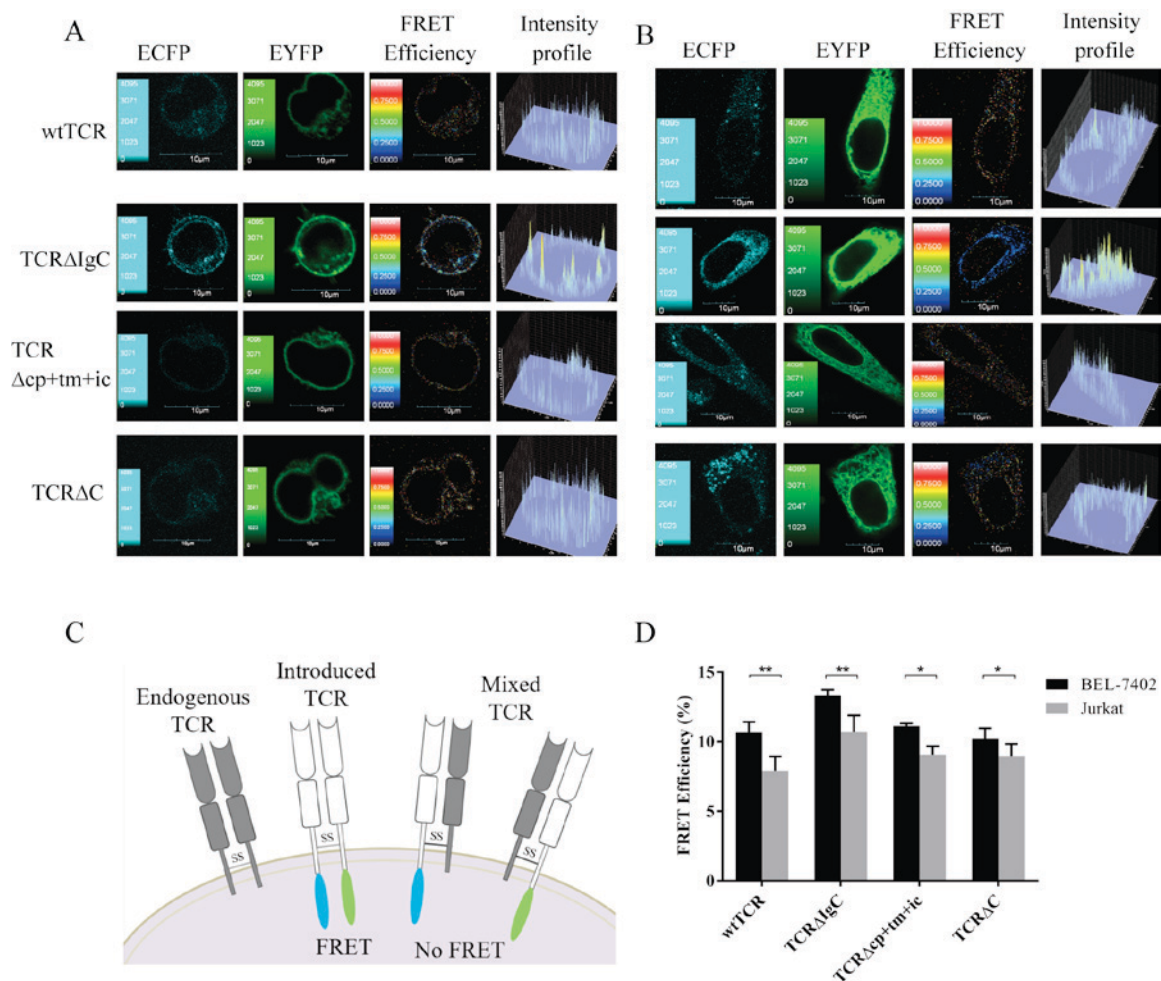


Figure 3. FRET efficiencies between chimeric TCR $\alpha$  and TCR $\beta$  chains. (A) Jurkat and (B) BEL-7402 cells transiently expressed wtTCR, TCR $\Delta$ IgC, TCR $\Delta$ cp+tm+ic and TCR $\Delta$ C. The confocal images in the ECFP and EYFP channels were performed with a confocal laser-scanning microscope and FV10-ASW 1.7 software. The FRET efficiency and intensity profile were calculated using the sensitized acceptor emission method. (C) Detection of FRET between TCR $\alpha$ -ECFP and TCR $\beta$ -EYFP when pairing. If mispairing occurred, no FRET was detected. (D) Four independent cell images in each group and five randomly selected regions of interest in each cell image were selected for statistical analysis of the FRET efficiency. Data are expressed as the mean  $\pm$  standard deviation. \* $P < 0.05$ , \*\* $P < 0.01$ . Data represent one of four independent experiments with similar results. Scale bar=10  $\mu$ m. The continuous color scale (black-white) represents FRET efficiency (0-1). TCR, T cell receptor; wt, wild-type; Ig, immunoglobulin-like; cp+tm+ic, connecting peptide, transmembrane and intracellular; FRET, fluorescence resonance energy transfer.

wtTCR and chimeric TCRs were co-cultured with the HepG2 (HLA-A<sup>2+</sup>, Huh-1 (HLA-A<sup>2+</sup>) and BEL-7402 (HLA-A<sup>2-</sup>) human hepatocellular carcinoma cell lines. The secretion of IFN- $\gamma$  into the medium was measured using an ELISA procedure. As shown in Fig. 4A, when co-cultured with HLA-A<sup>2+</sup> cell lines, the PBMCs transduced with TCR $\Delta$ IgC secreted the same quantity of IFN- $\gamma$  as the PBMCs transduced with wtTCR. Unexpectedly, the PBMCs transduced with TCR $\Delta$ cp+tm+ic and TCR $\Delta$ C secreted lower levels of IFN- $\gamma$ , compared with wtTCR, with levels close to those of the PBMCs containing no TCR transgene. This indicated that TCR $\Delta$ cp+tm+ic and TCR $\Delta$ C did not trigger cytokine secretion. The levels of IFN- $\gamma$  in the PBMCs transduced with the three chimeric TCRs or wtTCR were not above background levels following incubation with the HLA-A<sup>2-</sup> cell line.

The cell-mediated cytotoxicity of human PBMCs expressing either wtTCR or the modified TCR variants was also compared in a 4-h CAM release assay. The Ad5F35 adenoviruses encoding the wtTCR and chimeric TCRs were transferred into PBMCs. PBMCs expressing the wtTCR and

chimeric TCRs were co-cultured with CAM-labeled human hepatocellular carcinoma cell lines. It was observed that wtTCR and TCR $\Delta$ IgC were able to mediate specific lysis of the HLA-A<sup>2+</sup> hepatocellular carcinoma cell lines, as shown in Fig. 4B. The lymphocytes expressing TCR $\Delta$ IgC showed equivalent lysis in the HLA-A<sup>2+</sup> HepG2 and Huh-1 target cell lines, compared with the wtTCR at an E:T ratio of 30:1 (11.42 $\pm$ 0.75 and 12.03 $\pm$ 1.10%, respectively for HepG2 target cells; 11.10 $\pm$ 0.92 and 12.13 $\pm$ 1.17%, respectively for Huh-1 target cells). These results indicated that the lymphocytes expressing TCR $\Delta$ IgC exhibited similar cytotoxic activity to wtTCR. However, the lymphocytes expressing TCR $\Delta$ cp+tm+ic and TCR $\Delta$ C exhibited lower lytic activity, compared with the wtTCR, however, lysis was equivalent to the control PBMCs. In the HLA-A<sup>2-</sup> target cell line, no significant lysis was observed by any of the TCR transgene PBMCs.

Taken together, TCR $\Delta$ IgC substitution of the  $\gamma\delta$ TCR IgC domain was functionally equivalent to the wtTCR, whereas TCR $\Delta$ cp+tm+ic and TCR $\Delta$ C affected the recognition and cytotoxic abilities.

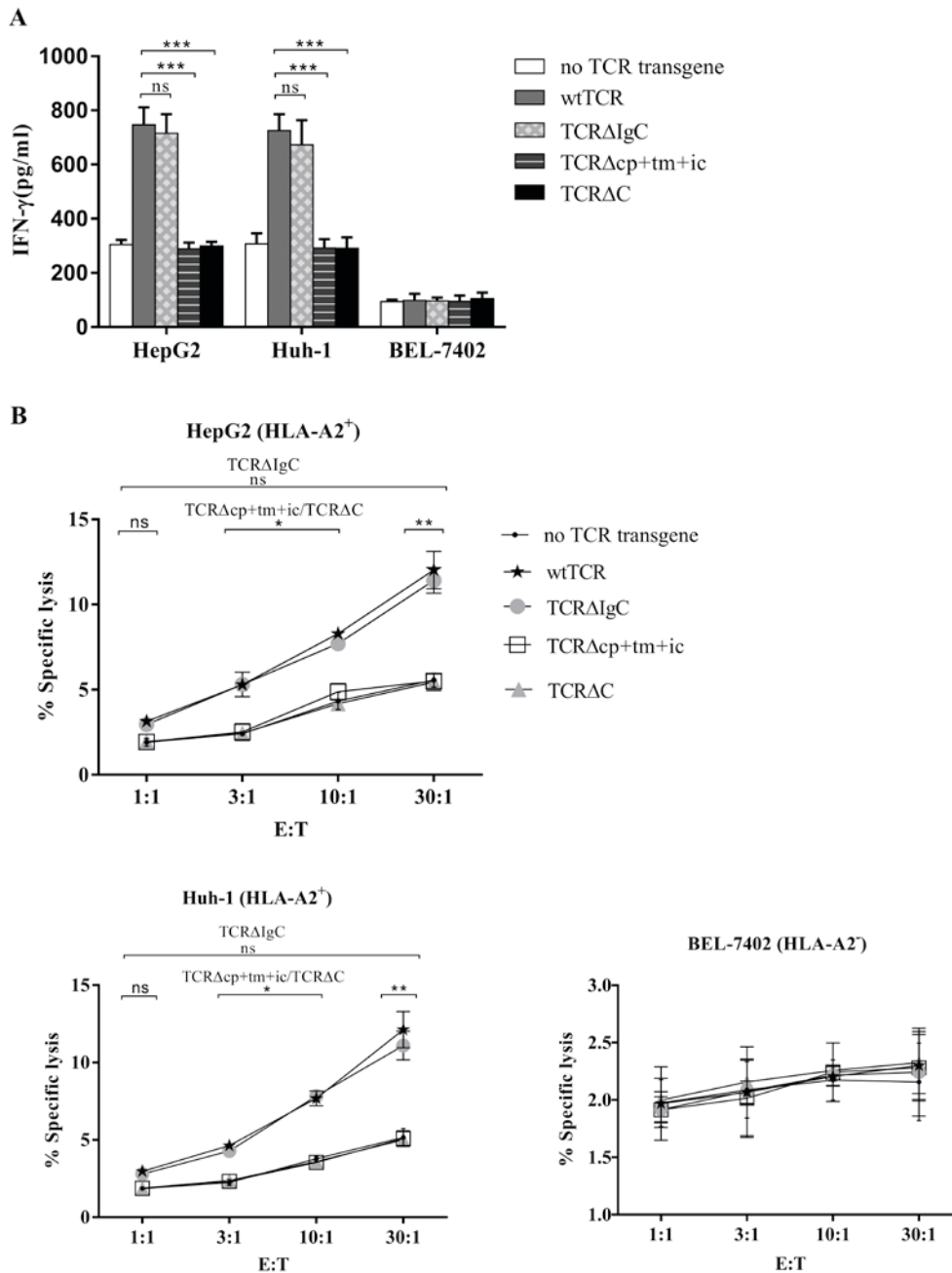


Figure 4. Function of chimeric TCRs in PBMCs. (A) Human PBMCs expressing either wtTCR or modified TCR variants were co-cultured with different tumor cell lines for 24 h, and concentrations of IFN- $\gamma$  secreted into the co-culture supernatant were measured using ELISA. (B) Specific cytotoxicity of tumor cell lines. The human PBMCs expressing the wtTCR, TCRAIgC, TCRAcp+tm+ic or TCRAC transgenes, or without a TCR transgene were co-cultured with CAM-labeled tumor cell lines at the indicated E:T ratios for 4 h, following which specific lysis was calculated. Results represent the average of three independent experiments, performed with three donors. \* $P < 0.05$ , \*\* $P < 0.01$ , \*\*\* $P < 0.001$ ). TCR, T cell receptor; PBMCs, peripheral blood mononuclear cells; wt, wild-type; Ig, immunoglobulin-like; cp+tm+ic, connecting peptide, transmembrane and intracellular; C, complete constant; CAM, calcein AM; IFN- $\gamma$ , interferon- $\gamma$ ; HLA, human leukocyte antigen; E:T, effector to target cell; ns, non-significant.

## Discussion

The  $\alpha\beta$  and  $\gamma\delta$ TCRs are two types of antigen receptor expressed on distinct T cell populations,  $\gamma\delta$ TCR is homologous to  $\alpha\beta$ TCR in the variable and constant regions, and the  $\alpha\beta$  and  $\gamma\delta$  TCRs are heterodimers linked by disulfide bonds (20). The  $\gamma\delta$ T cells carrying V $\gamma$ 9V $\delta$ 2 TCRs are primarily found in peripheral blood, where they constitute a minor fraction of total T cells and respond to non-peptidic intermediates of

the mevalonate pathway, termed phosphoantigens (21). It has been reported that V $\gamma$ 9V $\delta$ 2TCR can be efficiently expressed in  $\alpha\beta$ T cells without mispairing with  $\alpha\beta$ TCR, and mediates the tumor-specific proliferation of  $\alpha\beta$ T cells (17). In the present study, three chimeric TCR variants were generated by swapping the partial or complete constant regions of  $\alpha\beta$ TCR with those of  $\gamma\delta$ TCR (Fig. 1). These constructs were assessed for surface expression, mispairing with endogenous TCR chains, and TCR transgene-mediated functions in Jurkat T cells and



primary human T cells. The subsequent observations revealed for these chimeric TCR variants that the introduction of the  $\gamma\delta$ TCR IgC domain in the  $\alpha\beta$ TCR improved surface expression, reduced mispairing and did not compromise the function of the unmodified wtTCR. The other two TCRs containing cp+tm+ic or C domain of  $\gamma\delta$ TCR showed decreased mispairing with endogenous TCR, but impaired function in T cells.

FACS analysis in Jurkat cells showed that TCR $\Delta$ IgC exhibited improved surface expression, and the CLSM images also showed TCR $\Delta$ IgC exhibited on the cell surface of the Jurkat cells and the non-T cells (BEL-7402). The fluorescent images of the reporter were subjected to FRET analysis, which showed that TCR $\Delta$ IgC exhibited a higher FRET efficiency, compared with the wtTCR in BEL-7402 cells and Jurkat cells. Detailed statistical analysis of FRET efficiencies between BEL-7402 cells and Jurkat cells showed that TCR $\Delta$ IgC reduced mispairing, but failed to prevent mispairing with endogenous TCR. The function of TCR $\Delta$ IgC in cytotoxic lymphocytes showed equivalent IFN- $\gamma$  secretion and cytotoxic activity as in wtTCR when targeting HLA-A<sup>2+</sup> HepG2 and Huh-1 cell lines, however not the HLA-A<sup>2-</sup> cell line. These results suggested that the  $\gamma\delta$ TCR IgC domain substituted for  $\alpha\beta$ TCR preserved the recognition and lytic abilities of wtTCR, and even classic HLA restriction. The TCR  $\alpha\beta$  heterodimer has three conserved basic residues (R, K and K) in the transmembrane regions. These residues are considered to drive the associations between TCR and CD3 components by forming pair-wise ionic interactions, however, the association between this charged residue and the  $\alpha\beta$ TCR heterodimer remains to be elucidated (22). The present study hypothesized that TCR $\Delta$ IgC prevents mispairing with endogenous TCR to a certain extent, perhaps due to harboring the  $\gamma\delta$ TCR IgC domain, and the preserved ability of the original TCR may be due to the  $\alpha\beta$ TCR transmembrane region interacting with the CD3 complex.

By contrast, the TCR $\Delta$ cp+tm+ic and TCR $\Delta$ C did not increase the surface expression significantly, compared with the wtTCR when monitoring these TCR variants in living cells. No significant differences in FRET efficiencies were found for the TCR $\Delta$ cp+tm+ic and TCR $\Delta$ C, compared with the wtTCR in BEL-7402 cells and Jurkat cells. However, the statistical analysis of FRET efficiencies between BEL-7402 cells and Jurkat cells showed these two modified TCRs decreased mispairing. At present, the molecular mechanisms determining the efficiency of TCR pairing remain to be elucidated. Studies have shown that the variable region sequences are important in determining the efficiency of the expression of TCRs (23). In the present study, which examined TCR constant region modifications (TCR $\Delta$ cp+tm+ic and TCR $\Delta$ C), minimal effect was found in their expression efficiencies, compared with wtTCR. It was hypothesized that the variable region sequences drive efficient  $\alpha\beta$  pairing, which can proceed despite modifications in the constant region. Unexpectedly, when their function was assessed in cytotoxic lymphocytes, the present study observed that TCR $\Delta$ cp+tm+ic and TCR $\Delta$ C were unable to trigger the secretion of IFN- $\gamma$ , and failed to mediated cytotoxicity in either the HLA-A<sup>2+</sup> nor HLA-A<sup>2-</sup> hepatocellular carcinoma cell lines. The TCR $\beta$  chain contains a conserved transmembrane glutamic acid, which is not found in the  $\gamma$  chain, and this residue may be a key determinant in the differential CD3 composition of the  $\alpha\beta$  and  $\gamma\delta$  complexes (24).

The chimeric TCRs in the present study contained  $\gamma$  instead of  $\beta$  residues in the transmembrane domain, which may have affected the composition of the CD3 subunits. Therefore, the present study hypothesized that the differences in CD3 subunit composition between the  $\alpha\beta$ - and  $\gamma\delta$ TCR/CD3 complexes may have resulted in the chimeric TCRs containing a substituted cp+tm+ic domain of  $\gamma\delta$ TCR failing to transduce a signal through the TCR complex. This may explain why TCR $\Delta$ cp+tm+ic and TCR $\Delta$ C lost the functions of recognition and lysis in primary T cells.

In conclusion, the present study showed that the modified  $\alpha\beta$ TCR, substituted for by the IgC domain of  $\gamma\delta$ TCR, improved expression and pairing on the cell surface, and did not compromise the function of the already present wtTCR.

## Acknowledgements

This study was supported by the Medical Science and Technology Research Foundation of Guangdong Province (grant no. A2016041) and the National Natural Science Foundation of China (grant nos. 31300737 and 81303292) and the Natural Science Foundation of Guangdong Province (grant no. 2015A030310310).

## References

1. Sharpe M and Mount N: Genetically modified T cells in cancer therapy: Opportunities and challenges. *Dis Model Mech* 8: 337-350, 2015.
2. Casucci M, Hawkins RE, Dotti G and Bondanza A: Overcoming the toxicity hurdles of genetically targeted T cells. *Cancer Immunol Immunother* 64: 123-130, 2015.
3. Cameron BJ, Gerry AB, Dukes J, Harper JV, Kannan V, Bianchi FC, Grand F, Brewer JE, Gupta M, Plesa G, *et al*: Identification of a Titin-derived HLA-A1-presented peptide as a cross-reactive target for engineered MAGE A3-directed T cells. *Sci Transl Med* 5: 197ra103, 2013.
4. Johnson LA, Morgan RA, Dudley ME, Cassard L, Yang JC, Hughes MS, Kammula US, Royal RE, Sherry RM, Wunderlich JR, *et al*: Gene therapy with human and mouse T-cell receptors mediates cancer regression and targets normal tissues expressing cognate antigen. *Blood* 114: 535-546, 2009.
5. Parkhurst MR, Yang JC, Langan RC, Dudley ME, Nathan DA, Feldman SA, Davis JL, Morgan RA, Merino MJ, Sherry RM, *et al*: T cells targeting carcinoembryonic antigen can mediate regression of metastatic colorectal cancer but induce severe transient colitis. *Mol Ther* 19: 620-626, 2011.
6. Morgan RA, Chinnsamy N, Abate-Daga D, Gros A, Robbins PF, Zheng Z, Dudley ME, Feldman SA, Yang JC, Sherry RM, *et al*: Cancer regression and neurological toxicity following anti-MAGE-A3 TCR gene therapy. *J Immunother* 36: 133-151, 2013.
7. Linette GP, Stadtmauer EA, Maus MV, Rapoport AP, Levine BL, Emery L, Litzky L, Bagg A, Carreno BM, Cimino PJ, *et al*: Cardiovascular toxicity and titin cross-reactivity of affinity-enhanced T cells in myeloma and melanoma. *Blood* 122: 863-871, 2013.
8. van Loenen MM, de Boer R, Amir AL, Hagedoorn RS, Volbeda GL, Willemze R, van Rood JJ, Falkenburg JH and Heemskerk MH: Mixed T cell receptor dimers harbor potentially harmful neoreactivity. *Proc Natl Acad Sci USA* 107: 10972-10977, 2010.
9. Bendle GM, Linnemann C, Hooijkaas AI, Bies L, de Witte MA, Jorritsma A, Kaiser AD, Pouw N, Debets R, Kieback E, *et al*: Lethal graft-versus-host disease in mouse models of T cell receptor gene therapy. *Nat Med* 16: 565-570, 2010.
10. Cohen CJ, Zhao Y, Zheng Z, Rosenberg SA and Morgan RA: Enhanced antitumor activity of murine-human hybrid T-cell receptor (TCR) in human lymphocytes is associated with improved pairing and TCR/CD3 stability. *Cancer Res* 66: 8878-8886, 2006.

11. Cohen CJ, Li YF, El-Gamil M, Robbins PF, Rosenberg SA and Morgan RA: Enhanced antitumor activity of T cells engineered to express T-cell receptors with a second disulfide bond. *Cancer Res* 67: 3898-3903, 2007.
12. Voss RH, Willemsen RA, Kuball J, Grabowski M, Engel R, Intan RS, Guillaume P, Romero P, Huber C and Theobald M: Molecular design of the Calpha-beta interface favors specific pairing of introduced TCRalpha-beta in human T cells. *J Immunol* 180: 391-401, 2008.
13. Aggen DH, Chervin AS, Schmitt TM, Engels B, Stone JD, Richman SA, Piepenbrink KH, Baker BM, Greenberg PD, Schreiber H and Kranz DM: Single-chain V $\alpha$ V $\beta$  T-cell receptors function without mispairing with endogenous TCR chains. *Gene Ther* 19: 365-374, 2012.
14. Ochi T, Fujiwara H, Okamoto S, An J, Nagai K, Shirakata T, Mineno J, Kuzushima K, Shiku H and Yasukawa M: Novel adoptive T-cell immunotherapy using a WT1-specific TCR vector encoding silencers for endogenous TCRs shows marked antileukemia reactivity and safety. *Blood* 118: 1495-1503, 2011.
15. Provasi E, Genovese P, Lombardo A, Magnani Z, Liu PQ, Reik A, Chu V, Paschon DE, Zhang L, Kuball J, *et al*: Editing T cell specificity towards leukemia by zinc finger nucleases and lentiviral gene transfer. *Nat Med* 18: 807-815, 2012.
16. van der Veken LT, Coccoris M, Swart E, Falkenburg JH, Schumacher TN and Heemskerk MH: Alpha beta T cell receptor transfer to gamma delta T cells generates functional effector cells without mixed TCR dimers in vivo. *J Immunol* 182: 164-170, 2009.
17. Marcu-Malina V, Heijhuurs S, van Buuren M, Hartkamp L, Strand S, Sebestyen Z, Scholten K, Martens A and Kuball J: Redirecting  $\alpha\beta$  T cells against cancer cells by transfer of a broadly tumor-reactive  $\gamma\delta$ T-cell receptor. *Blood* 118: 50-59, 2011.
18. Tao C, Shao H, Yuan Y, Wang H, Zhang W, Zheng W, Ma W and Huang S: Imaging of T-cell receptor fused to CD3 $\zeta$  reveals enhanced expression and improved pairing in living cells. *Int J Mol Med* 34: 849-855, 2014.
19. Jang YY, Cho D, Kim SK, Shin DJ, Park MH, Lee JJ, Shin MG, Shin JH, Suh SP and Ryang DW: An improved flow cytometry-based natural killer cytotoxicity assay involving calcein AM staining of effector cells. *Ann Clin Lab Sci* 42: 42-49, 2012.
20. De Libero G, Lau SY and Mori L: Phosphoantigen presentation to TCR  $\gamma\delta$  Cells, a conundrum getting less gray zones. *Front Immunol* 5: 679, 2014.
21. Scheper W, Sebestyen Z and Kuball J: Cancer Immunotherapy using  $\gamma\delta$ T cells: Dealing with diversity. *Front Immunol* 5: 601, 2014.
22. Kuhns MS, Davis MM and Garcia KC: Deconstructing the form and function of the TCR/CD3 complex. *Immunity* 24: 133-139, 2006.
23. Heemskerk MH, Hagedoorn RS, van der Hoorn MA, van der Veken LT, Hoogeboom M, Kester MG, Willemze R and Falkenburg JH: Efficiency of T-cell receptor expression in dual-specific T cells is controlled by the intrinsic qualities of the TCR chains within the TCR-CD3 complex. *Blood* 109: 235-243, 2007.
24. Teixeira E, Daniels MA, Hausmann B, Schrum AG, Naeher D, Luescher I, Thome M, Bragado R and Palmer E: T cell division and death are segregated by mutation of TCRbeta chain constant domains. *Immunity* 21: 515-526, 2004.